Detection mechanism for quantum phase transition in superconducting qubit array

Ying-Dan Wang,[1,*] Fei Xue,[1,†] Zhi Song,[2] and Chang-Pu Sun[1]
[1]*Institute of Theoretical Physics, Chinese Academy of Sciences, Beijing 100080, China*
[2]*Department of Physics, Nankai University, Tianjin 300071, China*
(Received 29 May 2007; revised manuscript received 27 August 2007; published 27 November 2007)

We describe a mechanism to detect quantum phase transition (QPT) in a system by a coherent probe weakly coupled to it. We illustrate this mechanism by a circuit QED architecture where a superconducting Josephson junction qubit array interacts with a one-dimensional superconducting transmission line resonator (TLR). The superconducting qubit array is modeled as an Ising chain in transverse field. Our investigation shows that the QPT phenomenon in the superconducting qubit array can be evidently revealed by the correlation spectrum of TLR output: At the critical point, the drastic broadening of spectrum indicates the occurrence of QPT. We also show the generalization of this mechanism to other QPT systems.

DOI: 10.1103/PhysRevB.76.174519 PACS number(s): 74.81.Fa, 73.43.Nq, 42.50.Pq, 75.10.Pq

I. INTRODUCTION

Quantum phase transition (QPT) is essentially caused by quantum fluctuation at zero temperature.[1] Though the absolute zero temperature is not achievable in experiment, quantum critical behavior can be observed at very low temperature where the quantum fluctuation prevails. However, it is not straightforward to detect the quantum critical behavior which is usually masked by other degree of freedom in the complicated system. For example, the superconductivity conceals the direct study of the quantum order-disorder transition in high-T_c superconductors and in heavy-fermion materials, and the characterization of the zero temperature magnetic instability is complicated by the presence of charge carriers and substitutional disorder.[2] It is favorable to detect quantum critical behavior without direct measurement on the critical system itself. Recent theoretical investigations[3–6] have shown that ground state hypersensitivity near the critical point can result in the hypersensitivity in the time evolution of the QPT system, which has a profound relationship with quantum chaos as well as quantum decoherence. We find that these discoveries provide a possible mechanism for indirectly probing QPT, which may have broad applications.

In this paper, by a concrete physical system, we describe an indirect detection scheme in a macroscopic QPT system, the superconducting Josephson junction (JJ) qubit array which is modeled as an Ising chain in transverse field (ITF). The superconducting qubit array is coherently coupled to an on-chip superconducting transmission line resonator (TLR) via circuit QED architecture.[7] We find that, due to the dynamic hypersensitivity near the critical point, the critical behavior of this qubit array manifests itself in the exotic spectral structure of its coupled system. That is, when QPT occurs in the superconducting qubit array, the spectrum of the TLR is significantly changed from discrete-peak structure into a smooth and continuous distribution. The drastic broadening of the spectrum serves as a witness of QPT. In the last section of this paper, we also show that this mechanism can be applied to other QPT systems.

II. QUANTUM PHASE TRANSITION MODEL AND ITS ENERGY SPECTRUM

We consider a quantum network including N Cooper pair boxes (CPBs) (see Fig. 1). Each CPB is a direct current superconducting quantum interference device (dcSQUID) formed by a superconducting island connected to two Josephson junctions and αth CPB is biased by an external voltage $V^{g\alpha}$. The effective Josephson tunneling energy can be modified by the magnetic flux Φ_x threading the dcSQUID. When the coupling capacitance C_m between two CPBs is much smaller than the total capacitance C_Σ connected to each CPB (e.g., in Ref. 9, $C_m/C_\Sigma \approx 0.05$), we can only consider the nearest neighbor interaction, and the Coulomb energy of this CPB chain reads

$$H_C = E_c \sum_i (n^{(\alpha)} - n_g^{(\alpha)})^2 + E_m \sum_i (n^{(\alpha)} - n_g^{(\alpha)})(n^{(\alpha+1)} - n_g^{(\alpha+1)}), \tag{1}$$

where $E_c = 2e^2/C_\Sigma$, $E_m = 4e^2 C_m / C_\Sigma^2$, and $n^{(\alpha)}$ is the number of excess Cooper pairs on the αth CPB and $n_g^{(\alpha)} = V_g^{(\alpha)}/2e$. With proper bias voltage, the CPB behaves as a qubit[8] and the qubit array becomes an engineered "spin" chain with N spin-1/2 particles. Then, the qubit array can be described by a one-dimensional (1D) ITF model with the effective Hamiltonian

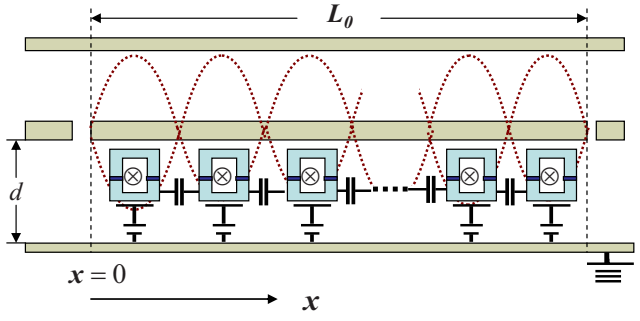

FIG. 1. (Color online) The schematics of our setup. A capacitively coupled Josephson junction qubit array is placed in a 1D TLR. Each qubit couples with the quantized magnetic field of the TLR.

$$H_0 = \hat{h}(\lambda) \equiv B\sum_{\alpha=1}^{N} (\lambda\sigma_x^{(\alpha)} + \sigma_z^{(\alpha)}\sigma_z^{(\alpha+1)}), \tag{2}$$

where $\lambda = B_x/B$ and $B = e^2 C_m / C_\Sigma^2$ characterize the Coulomb interaction between the nearest neighbors. The σ_x-dependent part comes from the Josephson energy of each CPB $B_x = E_J \cos(\pi\Phi_x/\Phi_0)/2$, with E_J the Josephson energy of single junction and $\Phi_0 = h/2e$ the flux quantum. Here, all CPBs are assumed to be identical and biased at the optimal point. The Pauli matrix operators

$$\sigma_z = |0\rangle\langle 0| - |1\rangle\langle 1|,$$

$$\sigma_x = -|0\rangle\langle 1| - |1\rangle\langle 0| \tag{3}$$

are defined in terms of the charge eigenstates of operator n $|0\rangle$ and $|1\rangle$. $|0\rangle$ and $|1\rangle$ denote 0 and 1 excess Cooper pair on the island, respectively. Note that this qubit array is completely different from the generic JJ array, which is usually used to study the superfluid-Mott insulator phase transition.[3] Until recently, the research of Josephson junction extends to qubit regime, and several superconducting Josephson junction qubits array configurations have been investigated for unpaired Majorana fermion states[10] and quantum state transfer.[11,12] Experimentally, a most recent experiment has demonstrated the possibility to implement a four-JJ-qubit Ising array.[13]

In our setup, as a quantum probe, a 1D TLR of length L_0, is placed in parallel with this qubit array (see Fig. 1). The distance between the center superconducting line and the line connected with qubit is d. Each CPB is situated at the antinodes

$$x = \frac{(2n+1)L_0}{2N} \quad (n = 0, \ldots, N-1) \tag{4}$$

of the magnetic field induced by the oscillating supercurrent in the TLR.[7] Since the current vanishes at the end of the TLR, this provides the boundary condition for the electromagnetic field of this on-chip resonator. Thus, the electric field is zero at those antinodes, and the qubits are only coupled with the magnetic component which shifts the original Φ_x threading each dcSQUID by

$$\Phi' = \frac{\eta\Phi_0}{\pi}(a + a^\dagger), \tag{5}$$

with

$$\eta = \frac{\pi S_0}{d\Phi_0}\sqrt{\frac{\hbar l\omega}{L_0}}, \tag{6}$$

where l is the inductance per unit length and S_0 is the enclosed area of the dcSQUID. For very large N, the energy spectrum of the cavity mode is quasicontinuous. In principle, it is hard to single out one mode especially when the two systems are not exactly resonant. However, if we take the dissipation for the cavity into account, there are only some discrete Fox-Li quasimodes surrounded by many additional modes. The additional modes induce the decay of the Fox-Li quasimode with decay rate Γ. Therefore, the single mode approximation is still hold. Here, we have assumed that only a single mode (it is worth to point out that our proposal here is also valid for multimode field) with frequency ω is coupled with qubit array and a ($a^\dagger$) is its annihilation (creation) operator.

Usually, η is small enough for the harmonic approximation[3,14] $\cos(\eta(a+a^\dagger)) \approx 1 - \eta^2(a+a^\dagger)^2/2$. The extra flux modifies B_x in Eq. (2) to

$$B_x \cong \frac{E_J}{2}\left[1 - \left(\frac{\pi S}{\Phi_0 d}\sqrt{\frac{\hbar l\omega}{L}}(a + a^\dagger)\right)^2\right]. \tag{7}$$

This results in an additional coupling between the x component of the qubits and the bosonic mode,

$$H_I = -\frac{B\lambda\eta^2}{4}\sum_{\alpha}(a^\dagger a + aa^\dagger)\sigma_x^{(\alpha)}, \tag{8}$$

besides the free Hamiltonian of the bosonic mode $H_F = \omega a^\dagger a$. Here, we have already invoked the rotating wave approximation to neglect the high frequency terms proportional to $a^{\dagger 2}$ and a^2 under the condition $\omega \gg B_x, B$. This approximation can be satisfied with accessible parameters in the current experiments. For example, if we take[15] $C_\Sigma \sim 600$ aF, $C_m \sim 30$ aF, $L_0 \sim 1$ cm, $S_0 \sim 10$ μm^2, $d \sim 1$ μm, and $N = 500$, then $B = 1.6$ GHz, $E_J = 13$ GHz, $\omega \sim 120$ GHz, and $\eta \sim 0.1$.

Introducing the Jordan-Wigner transformation,

$$\sigma_z^{(\alpha)} = \prod_{\beta<\alpha}(2c_\beta^\dagger c_\beta - 1)(c_\alpha + c_\alpha^\dagger),$$

$$\sigma_x^{(\alpha)} = 1 - 2c_\alpha^\dagger c_\alpha, \tag{9}$$

the free Hamiltonian H_0 can be diagonalized as

$$H_0 = \sum_k \varepsilon_k\left(\gamma_k^\dagger\gamma_k - \frac{1}{2}\right) \tag{10}$$

by the fermionic quasiparticle operator

$$\gamma_k = \sum_{\alpha=1}^{N}\frac{e^{-ik\alpha}}{\sqrt{N}}\left(c_\alpha \cos\frac{\theta_k}{2} - ic_\alpha^\dagger \sin\frac{\theta_k}{2}\right), \tag{11}$$

with dispersion relation

$$\varepsilon_k(\lambda) = 2B\sqrt{1 + \lambda^2 - 2\lambda\cos k} \tag{12}$$

and

$$\tan\theta_k(\lambda) = \frac{\sin k}{\lambda - \cos k}. \tag{13}$$

The ground state $|G\rangle$ of H_0 describes the state without any quasiparticle excitation.[1,16,17]

With respect to the Fock state $|n\rangle$ of the TLR, the Hamiltonian of the whole system $H = H_0 + H_F + H_I$ can be decomposed as $H = \Sigma_n H_n |n\rangle\langle n|$, where each branch Hamiltonian

$$H_n \equiv \hat{h}(\lambda_n) = B\sum_{\alpha=1}^{N} (\lambda_n \sigma_x^{(\alpha)} + \sigma_z^{(\alpha)}\sigma_z^{(\alpha+1)}), \tag{14}$$

with $\lambda_n = \lambda[1-(2n+1)\eta^2/4]$. Here, the constant term $\hbar n\omega$ has been omitted. For further convenience, we introduce the pseudospin operators[18]

$$s_{xk} = i(\gamma_{-k}\gamma_k + \gamma_{-k}^{\dagger}\gamma_k^{\dagger}),$$

$$s_{yk} = \gamma_{-k}^{\dagger}\gamma_k^{\dagger} - \gamma_{-k}\gamma_k,$$

$$s_{zk} = \gamma_k^{\dagger}\gamma_k + \gamma_{-k}^{\dagger}\gamma_{-k} - 1. \tag{15}$$

They describe the pairing of quasiparticle excitations of γ_k. In terms of pseudospin operators $\mathbf{S}_k = (s_{xk}, s_{yk}, s_{zk})$, each branch Hamiltonian

$$H_n = \sum_{k>0} \mathbf{B}_{nk} \cdot \mathbf{S}_k \tag{16}$$

describes a collection of pseudospins and each spin experiences different effective magnetic field

$$\mathbf{B}_{nk} = (\varepsilon_{nk} \sin 2\alpha_{nk}, 0, \varepsilon_{nk} \cos 2\alpha_{nk}), \tag{17}$$

with $2\alpha_{nk} = \theta_{nk} - \theta_k$, $\varepsilon_{nk} = \varepsilon_k(\lambda_n)$, and $\theta_{nk} = \theta_k(\lambda_n)$.

III. DETECTION OF QUANTUM PHASE TRANSITION BASED ON CIRCUIT QED

We expect to detect the critical behavior of the superconducting qubit array by the coherence property of the TLR. To do this, a natural option is to examine the correlation spectrum $S(\omega) = \int dt e^{-i\omega t} S(t)$, which is the Fourier transformation of the first-order correlation function of the single mode field,

$$S(t) = \langle a^{\dagger}(t)a(0)\rangle = \sum_n n|c_n|^2 e^{-\Gamma|t|} D_{n,n-1}(t). \tag{18}$$

Here, the average $\langle \cdots \rangle$ is taken over an initial state $|\Psi(0)\rangle = |\psi_0\rangle \otimes |G\rangle$, and $|\psi_0\rangle = \Sigma_n c_n |n\rangle$ is an arbitrary pure state of the TLR (discussion can also be generalized to the mixed state of TLR). The decoherence factor

$$D_{n,n-1}(t) = \langle G|\exp(iH_n t)\exp(-iH_{n-1}t)|G\rangle \tag{19}$$

evaluates the overlap of the wave functions driven by two different Hamiltonians H_n and H_{n-1} separately. We also phenomenologically introduce the decaying factor $\exp(-\Gamma|t|)$ in the quasimode treatment of dissipation, where Γ is about 6.3 MHz for the first excitation mode.[7]

With these knowledge, the spectral function

$$S(\omega) = \sum_n n|c_n|^2 D_{n,n-1}(\omega) \tag{20}$$

can be analytically derived (see Appendix) with

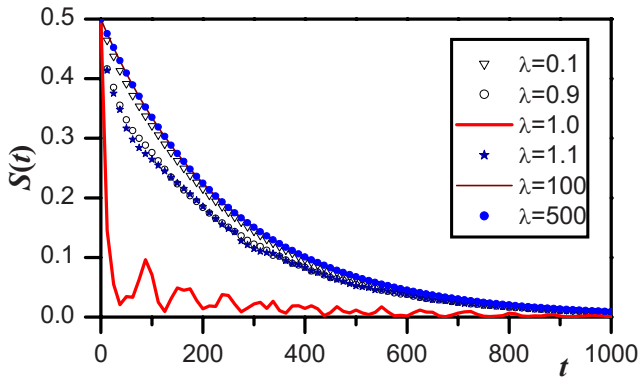

FIG. 2. (Color online) The first-order correlation function $S(t)$ for $|\psi_0\rangle = (|0\rangle + |1\rangle)/\sqrt{2}$ is plotted with different λ. Here, $N=1000$ and the time t is in the units of $1/B$.

$$D_{n,n-1}(\omega) = \sum_{a_k,b_k} F^{(n)}(\{a_k,b_k\}) L(\omega, \Omega^{(n)}(\{a_k,b_k\}), \Gamma). \tag{21}$$

Here, the sum is taken over all the possible configurations of combinations $\{(a_k,b_k)|a_k,b_k = \pm\}$, e.g., one possible combination is $\{(+,-)_1,(+,+)_2,\ldots,(-,+)_{N/2}\}$, and

$$F^{(n)}(\{a_k,b_k\}) = \prod_k c_{a_k b_k,k}^{(n,n-1)} \tag{22}$$

is defined by

$$c_{++=,k}^{(n,n-1)} = -\sin\alpha_{nk}\cos\alpha_{n-1k}\sin\Omega_{nk},$$

$$c_{+-,k}^{(n,n-1)} = \sin\alpha_{nk}\sin\alpha_{n-1k}\cos\Omega_{nk},$$

$$c_{-+,k}^{(n,n-1)} = \cos\alpha_{nk}\cos\alpha_{n-1k}\cos\Omega_{nk},$$

$$c_{--,k}^{(n,n-1)} = \cos\alpha_{nk}\sin\alpha_{n-1k}\sin\Omega_{nk}, \tag{23}$$

where $\Omega_{nk} = \alpha_{n-1k} - \alpha_{nk}$. Note that $D_{n,n-1}(\omega)$ is a sum of many Lorentzian distributions

$$L(\omega,\Lambda,\Gamma) = \frac{2\Gamma}{\Gamma^2 + (\omega-\Lambda)^2}, \tag{24}$$

with the same half-width Γ at half maximum but different central frequencies

$$\Omega^{(n)}(\{a_k,b_k\}) = \sum_k (a_k\varepsilon_{nk} + b_k\varepsilon_{n-1,k}). \tag{25}$$

Neglecting the decay of quasimodes, those Lorentzian line shapes reduce to delta functions.

The time evolution of the first-order correlation function $S(t)$ with $N=1000$ is shown in Fig. 2 for different λ with $|\psi_0\rangle = (|0\rangle + |1\rangle)/\sqrt{2}$. It can be seen that the decay rates for different λ are almost the same except $\lambda = 1$. This decay is induced by the dissipation of the quasimodes, which has the same influence for different λ. However, near the critical point, i.e., $\lambda \approx 1$, the decay is drastically enhanced. This means that there exists an extra strong decay mechanism related to QPT.

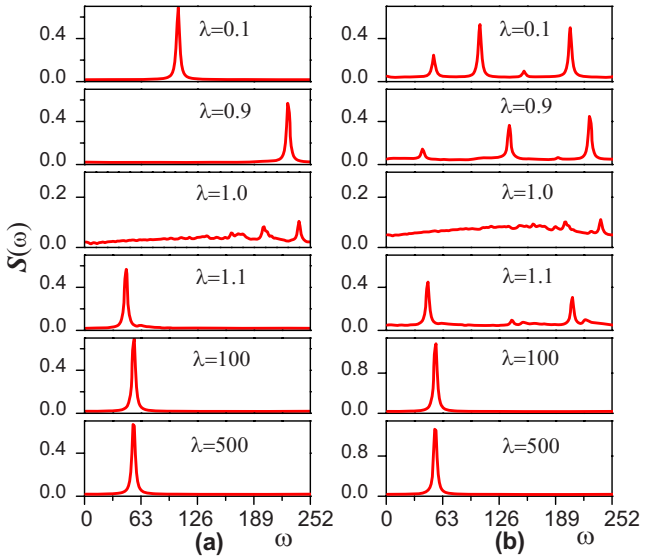

FIG. 3. (Color online) The spectrum $S(\omega)$ is shown with different λ. The left panel is for $|\psi_0\rangle=(|0\rangle+|1\rangle)/\sqrt{2}$ and the right panel is for a coherent state $|\psi_0\rangle=|\alpha\rangle$. Note that the vertical scale for $\lambda=1$ is different. Here, $N=1000$ and the frequency ω is in the units of 10^3B.

To illustrate the effect of QPT more clearly, we resort to the behavior of the spectral function $S(\omega)$. The numerical result by fast Fourier transformation is shown in Figs. 3 and 4. In Fig. 3, the left panel is for $|\psi_0\rangle=(|0\rangle+|1\rangle)/\sqrt{2}$, while the right panel is for a coherent state $|\psi_0\rangle=|\alpha\rangle$ with $\alpha=1$. It can be seen that, for the two different initial states, generally, there are only one or a few Lorentzian peaks centered at discrete frequencies in $S(\omega)$, while near the phase transition point, the spectrum of TLR gets broad and chaotic. As N increases, this broadened distribution at the critical point becomes more and more smooth and tends to be a white-noise spectrum at large N limit (see Fig. 4). Thus, the QPT of the superconducting qubit array is featured by the intensive

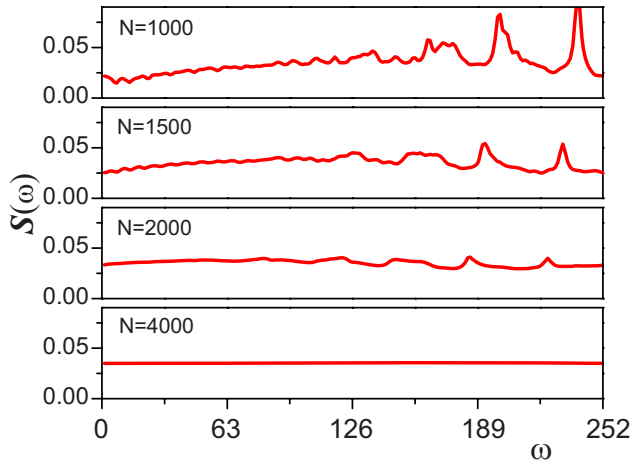

FIG. 4. (Color online) The spectrum $S(\omega)$ at the critical point is plotted for different N with $|\psi_0\rangle=(|0\rangle+|1\rangle)/\sqrt{2}$. The frequency ω is in the units of 10^3B.

broadening in the TLR output spectrum. Therefore, we can infer the QPT from the correlation spectrum of the quantum probe.

IV. UNDERLYING PHYSICS FOR THE SPECTRUM STRUCTURE

To investigate the underlying physical mechanism for the behavior described above, we rewrite $S(\omega)$ in the form

$$S(\omega)=\sum_{n,ii'} p_{i,i'}^{(n)}\langle E_i^{(n)}|E_{i'}^{(n-1)}\rangle L(\omega,\Lambda_{ii'}^{(n)},\Gamma). \tag{26}$$

Here, $|E_i^{(n)}\rangle$ is the ith eigenvector of H_n with eigenvalue $E_i^{(n)}$,

$$p_{i,i'}^{(n)}=n|c_n|^2\langle G|E_i^{(n)}\rangle\langle E_{i'}^{(n-1)}|G\rangle. \tag{27}$$

In a sense, $S(\omega)$ measures how many different eigenvectors of H_{n-1} are necessary to express one eigenvector of H_n. Due to the inner product in $p_{i,i'}^{(n)}$, the main contribution comes from the low excited energy eigenvectors. The more are necessary, the wider the support of $S(\omega)$. This observation provides the intrinsic reason for the broadening of the spectrum. Since η^2 is assumed to be a small perturbation, one would generally expect that the difference between H_n and H_{n-1} is almost negligible and their eigenvectors are very close to each other; this means

$$\langle E_i^{(n)}|E_{i'}^{(n-1)}\rangle\approx\delta_{i,i'} \tag{28}$$

and $S(\omega)$ reduces to a single Lorentzian distribution. Then, the support of $S(\omega)$ is very narrow and the corresponding inverse Fourier transformation $S(t)$ decays very slow.

However, the above analysis is invalid at the critical point. Near the critical point, the property of the QPT system, such as ground state and long range order, is significantly influenced by a small perturbation in either of the two competing terms: the Ising interaction and the transverse field. The seemingly very small difference between the two Hamiltonians H_n and H_{n-1} actually has drastic impact on the evolutions driven by the two Hamiltonians. This is the so-called hypersensitivity of QPT.[5] The dynamical hypersensitivity is related to the hypersensitivity of ground state in QPT system.[6] This implies that more eigenvectors of H_{n-1} are needed to reproduce one eigenvector of H_n. Therefore, many Lorentzian shapes have to be included, and the support of $S(\omega)$ becomes much broader. This, in turn, accelerates the decay of $S(t)$ and acts as the extra strong decay mechanism related to QPT as we have noticed in Fig. 2.

A more straightforward explanation of the spectral structure comes from the pseudospin Hamiltonian [Eq. (16)]. Far from the critical point, $\cos\alpha_{nk}\approx 1$ and $\sin\alpha_{nk}\approx 0$. This means that all the effective magnetic fields for different pseudospins are pointing to a single direction z and then all the pseudospins are aligned to form a large collective spin with identical precession frequency. In this case, although the number of qubits ($\sim N$) in the array is very large, all the qubits tend to stay in the same microscopic state (similar to the case of Bose Einstein condensation). Such ordered macroscopic "environment" will not destroy the coherence of the

coupled system. Then, the correlation spectrum exhibits discrete feature, which is the characteristic of highly coherent quantum system. However, near the critical point, the directions of local effective magnetic fields are not aligned and the pseudospins point to very different directions. Then, the collection of many pseudospins behaves as a random environment which results in a disorder or white-noise output spectrum of the coupled system.

Note that the above probe mechanism for QPT requires $B\eta^2 \gg \Gamma$, which ensures that the decoherence related to QPT near the critical point is far more prominent than that caused by the surrounding environment. However, the coupling coefficient $B\eta^2$ should also be much smaller than the energy scale of the free qubit array. Otherwise, the QPT nature of the ITF model would be significantly changed by the strongly coupled bosonic mode.

V. GENERAL FORMALISM

In the above sections, we show that the QPT of a CPB chain formed ITF model can be revealed by the correlation spectrum of a coupled transmission line resonator. As we analyzed in Sec. IV, this indirect detection scheme results from the hypersensitivity in the QPT dynamics, which is a rather general aspect of quantum phase transition. In this section, we give a general description of this detection method to various QPT models.

For a system that is a quantum phase transition model, then generally it has two competing terms,

$$H^{(q)} = H_1^{(q)} + H_2^{(q)}. \tag{29}$$

To probe the QPT of this system, it is weakly coupled to another detector with free Hamiltonian $H^{(d)}$ and interaction Hamiltonian H_I. The total Hamiltonian of the system is $H = H^{(q)} + H^{(d)} + H_I$. Suppose H_I has the following form:

$$H_I = gF^{(d)}P^{(q)}, \tag{30}$$

where $F^{(d)}$ is the dynamic variable of the detector system while $P^{(q)}$ is the dynamic variable of the QPT system. If the following two conditions are satisfied:

$$[H^{(d)}, F^{(d)}] = 0, \tag{31}$$

$$[H_1^{(q)}, P^{(q)}] = 0 \text{ or } [H_2^{(q)}, P^{(q)}] = 0, \tag{32}$$

we can detect QPT from correlation function

$$S^{(d)}(t) = \langle V_+^{(d)}(t) V_-^{(d)}(0) \rangle, \tag{33}$$

where $V_+^{(d)}$ ($V_-^{(d)}$) is the raising (lowering) operator for the eigenstate of $F^{(d)}$, i.e.,

$$V_\pm^{(d)}|f\rangle = (f \pm 1)|f\rangle, \tag{34}$$

and the average is carried out for a thermal state

$$\rho = \sum_f P_f |f\rangle\langle f| \otimes |\Psi_0\rangle\langle\Psi_0|. \tag{35}$$

Here, $|\Psi_0\rangle$ is the ground state of $H^{(q)}$ and $\{|f\rangle\}$ is the common eigenvectors of $F^{(d)}$ and $H^{(d)}$, with $F^{(d)}|f\rangle = f|f\rangle$ and $H^{(d)}|f\rangle = E_f^{(d)}|f\rangle$.

In this case,

$$S^{(d)}(t) = \langle V_+^{(d)}(t) V_-^{(d)}(0) \rangle \equiv \sum_f P_f D_{f,f-1}(t), \tag{36}$$

with

$$D_{f,f-1}(t) = \langle \Psi_0 | e^{iH_f t} e^{-iH_{f-1}t} | \Psi_0 \rangle. \tag{37}$$

Here, we have already used the relation

$$H = \sum_f H_f |f\rangle\langle f|, \tag{38}$$

with

$$H_f = H^{(q)} + gfP^{(q)} + E_f^{(d)}. \tag{39}$$

The spectral function can be written as

$$S(\omega) = \sum_f P_f \sum_{ii'} T_{f,f-1}^{i,i'} \langle E_{i,f} | E_{i',f-1} \rangle \delta(\omega + E_{i',f-1} - E_{i,f}), \tag{40}$$

where $T_{f,f-1}^{i,i'} \equiv \langle \Psi_0 | E_{i,f} \rangle \langle E_{i',f-1} | \Psi_0 \rangle$ and $|E_{i,f}\rangle$ is the ith eigenvector of H_f, i.e., $H_f|E_{i,f}\rangle = E_{i,f}|E_{i,f}\rangle$. As we discussed in Sec. IV, the number of peaks (δ functions) is mainly determined by the inner product $\langle E_{i,f} | E_{i',f-1} \rangle$. If the difference between H_f and H_{f-1} is negligible, only one term $i = i'$ is kept in the sum. Conversely, if the difference is large, there are many terms kept and many peaks in the spectrum. What determines the difference between H_f and H_{f-1} is the term $gfP^{(q)}$, which represents the influence of the detector. Suppose gf is small ($g \ll 1$ for weak coupling and the population on large f levels are usually very small), this term is not important when the QPT system is far away from the critical point. However, near the critical point, a small perturbation added on the two competitive terms results in major difference on the property of the system. The major difference of the system demonstrates itself through the spectral function of the detector, i.e., the spectral function exhibits multipeaks structure near the critical point.

To understand the above general formalism, we illustrate it with two specific examples.

(1) If $F^{(d)}$ is a generalized coordinate operator, such as $x, \theta, \ldots$, its conjugate variable is the generalized momentum $\Pi^{(d)}$, such as p_x, n.

Then the raising (lowering) operator can be written as

$$V_\pm^{(d)} = e^{\pm i\Pi^{(d)}}. \tag{41}$$

Or we can also use scaled raising (lowering) operator to simplify expression in some cases,

$$V_+^{(d)} = \sqrt{F^{(d)}} e^{i\Pi^{(d)}},$$

$$V_+^{(d)} = e^{-i\Pi^{(d)}} \sqrt{F^{(d)}}. \tag{42}$$

A concrete example of this kind is the number operator used in our paper, where $F^{(d)} = a^\dagger a$ and $V_+^{(d)} = a^\dagger$, $V_+^{(d)} = a$.

(2) If $F^{(d)}$ is the z component of an angular momentum operator, such as σ_z, $J_z, \ldots$, then the raising (lowering) operator can be written as

$$V_{\pm}^{(d)} = \sigma_{\pm} \quad \text{or } J_{\pm}. \tag{43}$$

This is the model studied in Ref. 5. The intrinsic reason of the deep valley in Figs. 2 and 3 of Ref. 5 is just what we discussed in this paper.

VI. SUMMARY AND REMARKS

In summary, with a superconducting circuit QED structure, we demonstrate an indirect detection scheme for the QPT phenomenon in a macroscopic quantum system. The quantum criticality of a superconducting qubit array can be probed by examining the coherent output of the coupled TLR. The detection mechanism utilizes the hypersensitivity of QPT system at the critical point. If one of the two competing terms in their Hamiltonian is weakly coupled with an external quantum system, the effect of this weak coupling to the critical system is magnified by the hypersensitivity at the critical point. This, in turn, accelerates the decoherence of the coupled system, which can be detected via drastic change in the correlation spectrum of the coupled system. This mechanism is possible to be generalized to other QPT systems with similar characteristics.

It is also notable that the sensitivity of the overlap of ground state with respect to a small perturbation in parameters has been studied in many body physics as Anderson orthogonality catastrophe (AOC). It has been proven that AOC coincides with the critical behavior of QPT for a certain category of physical model including ITF model discussed here.[6] One can expect that our detection scheme may also indicate the occurrence of AOC in this model.

On the other hand, we would like to remind the readers that a simple energy level crossing (SELC) may also lead to the same spectrum broadening since this dynamical behavior depends on the energy level structure of the system. Enhanced decoherence is essentially due to the large degree of freedom of the environment, while an environment with energy gap sufficiently large will suppress the decoherence. In the present example of transverse Ising model, the drastic broadening only occurs at the quantum critical point which is not a SELC point. In the case of SELC, there are energy gaps at both sides of the cross point. In many systems, the SELC of the ground and the first excited states is accompanied by the change in the low-lying spectral structure, which would induce enhanced decoherence. However, if the ground state and the first excited states are separated from other low-lying eigenstates by sufficient large energy gap, SELC does not lead to enhanced decay.[19] In this sense, this proposal might also be sensitive to SELC in some many-body systems.

Note added. Recently, we found an experimental work on probing quantum phase of ultracold atoms in optical lattices by transmission spectrum in cavity QED.[20] It is closely related to our proposal.

ACKNOWLEDGMENTS

Y.D.W. would like to thank Paolo Zanardi for his helpful instructions on dynamic instability of QPT in private communication. This work is funded by NSFC with Grant No. 90203018, No. 10474104, and No. 60433050 and NFRPC with No. 2001CB309310 and No. 2005CB724508.

APPENDIX: EVALUATION OF THE SPECTRAL FUNCTION

With pseudospin operators, the unperturbed Hamiltonian is written as

$$H_0 = \sum_k \varepsilon_k \left(\gamma_k^{\dagger} \gamma_k - \frac{1}{2} \right) = \sum_{k>0} \varepsilon_k s_{zk}, \tag{A1}$$

and the branch Hamiltonian is written as

$$H_n = \sum_{k>0} \varepsilon_{nk} s_{zk}^{(n)}, \tag{A2}$$

where

$$s_{zk}^{(n)} = s_{zk} \cos 2\alpha_{nk} + s_{xk} \sin 2\alpha_{nk}. \tag{A3}$$

Defining $|\pm\rangle_k$ ($|\pm\rangle_{nk}$) to be the eigenvector of the s_{zk} ($s_{zk}^{(n)}$) with eigenvalue ± 1, then the relations between the two sets of eigenvectors are

$$|-\rangle_{nk} = \cos \alpha_{nk} |-\rangle_k - \sin \alpha_{nk} |+\rangle_k,$$

$$|+\rangle_{nk} = \sin \alpha_{nk} |-\rangle_k + \cos \alpha_{nk} |+\rangle_k. \tag{A4}$$

Note that the inner products of different $|\pm\rangle_{nk}$ of different modes m, n are not orthogonal:

$${}_{mk}\langle \pm | \pm \rangle_{nk'} = \delta_{kk'} \cos(\alpha_{nk} - \alpha_{mk}),$$

$${}_{mk}\langle + | - \rangle_{nk'} = \delta_{kk'} \sin(\alpha_{mk} - \alpha_{nk}). \tag{A5}$$

The ground state of H_0 is a direct product of $|-\rangle_k$ as

$$|G\rangle = \prod_{k>0}^{\otimes} |-\rangle_k = \prod_{k>0}^{\otimes} (\cos \alpha_{nk} |-\rangle_{nk} - \sin \alpha_{nk} |+\rangle_{nk}), \tag{A6}$$

and its time evolution under the branch Hamiltonian can be calculated as

$$\exp(-iH_n t)|G\rangle = \prod_{k>0}^{\otimes} (\cos \alpha_{nk} e^{i\varepsilon_{nk}t} |-\rangle_{nk} + \sin \alpha_{nk} e^{-i\varepsilon_{nk}t} |+\rangle_{nk}). \tag{A7}$$

Inserting this relation into Eq. (19), it is straightforward reaching

$$D_{n,n-1}(t) = \prod_k \sum_{a_k b_k = \pm} (C_{a_k b_k,k}^{(n,n-1)} e^{i(a\varepsilon_{nk} + b\varepsilon_{n-1,k})t}) e^{-\Gamma|t|}, \tag{A8}$$

where we have included the decay caused by quasimode and the definition of $C_{ab,k}^{(n,n-1)}$ is the same as Eq. (23). Commuting the order of sum and product in the above equation, we get

$$D_{n,n-1}(t) = \sum_{\{(a_k,b_k)\}} \prod_k (C^{(n,n-1)}_{a_k b_k,k} e^{i(a\varepsilon_{nk}+b\varepsilon_{n-1,k})t}) e^{-\Gamma|t|} \equiv \sum_{\{(a_k,b_k)\}} D^{n,n-1}_{\{(a_k,b_k)\}}(t), \tag{A9}$$

where

$$D^{n,n-1}_{\{(a_k,b_k)\}}(t) = F^{(n)}(\{a_k,b_k\}) \exp\left(-\Gamma|t| + i\sum_k (a_k\varepsilon_{nk} + b_k\varepsilon_{n-1,k})t\right)$$

and $\{(a_k,b_k)\}$ is a set of configurations for the possible values of a and b in the product, such as $\{(+_1,-_1),(+_2,+_2),\ldots,(-_{2/N},+_{2/N})\}$. By performing Fourier transform on Eq. (A9) and inserting it into Eq. (20), we get the expression of spectral function $S(\omega)$ used in this paper,

$$S(\omega) = \sum_n n|C_n|^2 \sum_{\{(a_k,b_k)\}} D^{n,n-1}_{\{(a_k,b_k)\}}(\omega), \tag{A10}$$

with

$$D^{n,n-1}_{\{(a_k,b_k)\}}(\omega) = F^{(n)}(\{a_k,b_k\}) L(\omega,\Omega^{(n)}(\{a_k,b_k\}),\Gamma). \tag{A11}$$

*Present address: NTT Basic Research Laboratories, NTT Corporation, Atsugi-shi, Kanagawa 243-0198, Japan; wang@will.brl.ntt.co.jp

†Present address: Frontier Research System, The Institute of Physical and Chemical Research (RIKEN), Wako-shi, Saitama 351-0198, Japan.

[1] S. Sachdev, *Quantum Phase Transition* (Cambridge University Press, Cambridge, 1999).

[2] D. Bitko, T. F. Rosenbaum, and G. Aeppli, Phys. Rev. Lett. **77**, 940 (1996).

[3] J. Dziarmaga, A. Smerzi, W. H. Zurek, and A. R. Bishop, Phys. Rev. Lett. **88**, 167001 (2002).

[4] D. V. Khveshchenko, Phys. Rev. B **68**, 193307 (2003).

[5] H. T. Quan, Z. Song, X. F. Liu, P. Zanardi, and C. P. Sun, Phys. Rev. Lett. **96**, 140604 (2006).

[6] P. Zanardi and N. Paunkovic, Phys. Rev. E **74**, 031123 (2006); P. Zanardi, M. Cozzini, and P. Giorda, J. Stat. Mech.: Theory Exp. (2007) L02002.

[7] A. Wallraff, D. I. Schuster, A. Blais, L. Frunzio, R. S. Huang, J. Majer, S. Kumar, S. M. Girvin, and R. J. Schoelkopf, Nature (London) **431**, 162 (2004).

[8] Y. Nakamura, Y. A. Pashkin, and J. S. Tsai, Nature (London) **398**, 786 (1999).

[9] Y. A. Pashkin, T. Yamamoto, O. Astafiev, Y. Nakamura, D. V. Averin, and J. S. Tsai, Nature (London) **421**, 823 (2003); T. Yamamoto, Y. A. Pashkin, O. Astafiev, Y. Nakamura, and J. S. Tsai, *ibid.* **425**, 941 (2003).

[10] L. S. Levitov, T. P. Orlando, J. B. Majer, and J. E. Mooij, arXiv:cond-mat/0108266 (unpublished).

[11] A. Romito, R. Fazio, and C. Bruder, Phys. Rev. B **71**, 100501(R) (2005); A. Lyakhov and C. Bruder, New J. Phys. **7**, 181 (2005).

[12] M. Paternostro, G. M. Palma, M. S. Kim, and G. Falci, Phys. Rev. A **71**, 042311 (2005).

[13] M. Grajcar, A. Izmalkov, S. H. W. van der Ploeg, S. Linzen, T. Plecenik, Th. Wagner, U. Hubner, E. Il'ichev, H.-G. Meyer, A. Yu. Smirnov, P. J. Love, A. Maassen van den Brink, M. H. S. Amin, S. Uchaikin, and A. M. Zagoskin, Phys. Rev. Lett. **96**, 047006 (2006).

[14] Y. D. Wang, P. Zhang, D. L. Zhou, and C. P. Sun, Phys. Rev. B **70**, 224515 (2004).

[15] Y. D. Wang, Z. D. Wang, and C. P. Sun, Phys. Rev. B **72**, 172507 (2005).

[16] P. Pfeuty, Ann. Phys. (N.Y.) **57**, 79 (1970).

[17] E. Lieb, T. Schultz, and D. Mattis, Ann. Phys. (N.Y.) **16**, 407 (1961).

[18] P. W. Anderson, Phys. Rev. **112**, 1900 (1958).

[19] W. H. Zurek, U. Dorner, and P. Zoller, Phys. Rev. Lett. **95**, 105701 (2005).

[20] I. B. Mekhov, C. Maschler, and H. Ritsch, Nat. Phys. **3**, 319 (2007).